

Star-Shaped Poly(ether–ester) Block Copolymers: Synthesis, Characterization, and Their Physical Properties

Young Kweon Choi,[†] You Han Bae,[‡] and Sung Wan Kim*

Center for Controlled Chemical Delivery, Department of Pharmaceutics and Pharmaceutical Chemistry, University of Utah, Biomedical Polymers Research Building, Room No. 205, Salt Lake City, Utah 84112

Received July 7, 1998; Revised Manuscript Received October 19, 1998

ABSTRACT: Biodegradable polymers based on star-shaped poly(ethylene oxide) (PEO)–poly(L-lactide) (PLA) and PEO–poly(ϵ -caprolactone) (PCL) block copolymers were synthesized by a divergent synthetic method. Multiarm PEOs with various numbers of arms with a fixed molecular weight (MW \sim 10 000) were synthesized by anionic polymerization of ethylene oxide initiated with metalated plurifunctional initiators and used as a core block. The star-shaped block copolymers were prepared by ring-opening polymerization of L-lactide or ϵ -caprolactone in the presence of multiarm PEOs and a catalytic amount of stannous octoate. The equilibrium swelling and thermal and solution properties of the synthesized star-shaped polymers were examined. The block copolymers were swollen in distilled water, and the degree of swelling decreased as the number of arms increased. The melting point, crystallinity, and phase separation decreased with the degree of branching. A similar tendency in solution viscosity of the star-shaped PEO and block copolymers was found. The results obtained in this study revealed unique properties of star-shaped block polymers which could be useful in the formulation of delivery carrier for polypeptide.

Introduction

Recently, thermoplastic biodegradable hydrogels based on block copolymers have received attention for controlled drug delivery applications. They were designed by incorporation of water-soluble blocks into biodegradable, hydrophobic blocks to produce amphiphilic polymers. Casey et al.¹ synthesized ABA type triblock copolymers consisting of PEO (block B) and polyglycolide (PGA; block A) by ring-opening polymerization of glycolide initiated by end groups of PEO. The block copolymers formed a physically cross-linked hydrogel due to crystallization of PGA blocks. Similar systems consisting of PEO and other poly(α -hydroxy acids) have been reported by Cohn and Younes et al.² and Youxin et al.³ The block copolymers demonstrated controlled release of bovine serum albumin from a swollen PEO–PLA matrix over several weeks, where a smooth release pattern without burst effect in drug release was obtained. Although the PEO–poly(α -hydroxy acids) block copolymers have appropriate swelling properties for diffusion of proteins and polypeptides, PEO is nonbiodegradable and exhibits extraordinarily large hydrodynamic volume. This fact clearly limits the use of high molecular weights of PEO which may not be eliminated in the kidney, even though it is required for the better control of polymer composition governing hydration and mechanical property.

Star-shaped polymers exhibit a smaller hydrodynamic radius and lower solution viscosity when compared to linear polymers of the same molecular weight and composition. The smaller hydrodynamic radius of PEO is of importance in its complete renal excretion after

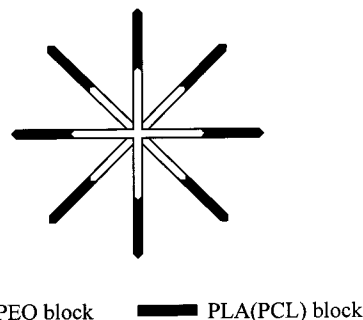


Figure 1. Schematic presentation of star-shaped PEO–PLA or PEO–PCL block copolymer structure (eight arms).

degradation of the polyester block. This may allow us to use a relatively high molecular weight multiarm PEO with a hydrodynamic radius small enough for renal excretion, for the synthesis of block copolymers with polyesters such as PLA and PCL.⁴

The objective of the present study is to synthesize and characterize star-shaped poly(ether–ester) block copolymers (Figure 1) and to investigate their architecture effect on the physical properties of swelling, solution viscosity, and thermal transition.

Experimental Section

Materials. Ethylene oxide was purchased from Fluka (Switzerland) and was distilled from potassium hydroxide and subsequently distilled from calcium hydride by a trap-to-trap distillation method, where a dry ice–acetone mixture was used for condensation of vaporized ethylene oxide. Poly(ethylene oxide)s (PEOs) with nominal molecular weights ranging from 1000 to 20 000 were purchased from Aldrich Chemicals Co. (Milwaukee, WI). Eight-arm PEO (MW 10 000) was purchased from Shearwater, Inc. (Huntsville, AL). All PEOs were dried by azeotropic distillation in benzene. L-Lactide was purchased from Polysciences Inc. (Warrington, PA) and was freshly purified by recrystallization in ethyl acetate and subsequent sublimation under vacuum. ϵ -Caprolactone was purchased from Aldrich, dried with calcium hydride, and distilled under

* To whom all correspondence should be addressed.

[†] Drug Delivery Research Laboratory, Sam Yang Pharmaceuticals R&D Center, 63-2 Hwaam-dong, Yusung-gu, Taejeon 305-348, Korea.

[‡] Department of Materials Science and Engineering, Kwangju Institute of Science and Technology, 572 Sangam-dong, Kwangsan-ku, Kwangju 506-712, Korea.

vacuum prior. These are purified prior to use. Trimethylolpropane (2-ethyl-2-hydroxymethyl-1,3-propanediol) and Pentaerythritol were obtained from Sigma (St. Louis, MO) and purified according to the procedures reported elsewhere.⁵ Potassium *tert*-butoxide (1.0 M solution in tetrahydrofuran), which was packaged under nitrogen in a Sure/Pac metal cylinder or Sure/Seal bottle, was obtained from Aldrich. Stannous octoate (stannous 2-ethylhexanoate) and acetyl chloride were obtained from Sigma and used without further purification. Potassium metal was obtained from Merck (Darmstadt, Germany). Tetrahydrofuran (THF) was distilled over lithium aluminum hydride and sodium metal, successively, and transferred to a reaction flask under nitrogen atmosphere prior to use. Deuterated solvents (CDCl_3 , 99.8 atom % D; $\text{DMSO}-d_6$, 100.0 atom % D) for NMR measurements were purchased from Aldrich. Molecular sieves (4 Å) were purchased from Mallinckrodt, Inc. (Paris, KY). All other reagents were an analytical grade and used without further purification.

Synthesis of Multiarm PEO. Three- and four-arm PEOs were prepared by anionic polymerization of ethylene oxide initiated with potassium alkoxides of trimethylolpropane and Pentaerythritol, respectively.

(a) *Trimethylolpropane Potassium Salt.* The three hydroxyl end groups of trimethylolpropane were transformed to potassium alkoxides by titration with potassium naphthylide in THF. Trimethylolpropane (1 mmol) was dissolved in 10 mL of dry THF, followed by titration with 0.1 M potassium naphthylide in THF, which was freshly prepared from an equimolar amount of potassium metal and naphthalene in dried THF at room temperature,⁶ under nitrogen atmosphere until a stable green color persisted for longer than 10 min. After calculating the initiator concentration from the amount of the titrant added, the solution was used for ethylene oxide polymerization without isolation step.

(b) *Potassium Pentaerythritolate.* Freshly prepared potassium *tert*-butoxide (200 mmol) was added into *tert*-butyl alcohol solution of Pentaerythritol (0.05 mol), and the mixture was stirred overnight at room temperature. The precipitate was obtained by pouring into an excess amount of anhydrous diethyl ether. After washing with diethyl ether, the product was dried under reduced pressure and stored in a vacuum desiccator until use.

(c) *Ethylene Oxide Polymerization.* Three-arm PEO was prepared by anionic polymerization of ethylene oxide initiated with trimethylolpropane potassium salt. After collecting a predetermined amount (10 mL, 0.197 mol) of ethylene oxide from distillation in a graduated cylinder, it was transferred into a reaction flask, flamed, and preevacuated prior to use by the trap-to-trap method. The THF solution of trimethylolpropane potassium salts (0.827×10^{-4} mol) was then introduced into the reaction flask with a Gastight syringe (Aldrich Co.) under reduced pressure. The ratio of monomer concentration to initiator was 225:1 to yield a PEO of molecular weight of 10 000. The final monomer concentration was adjusted to be 2 M by adding freshly dried THF and then subjected to polymerization for 3 days at 40 °C. The polymerization was terminated by adding an excess amount (relative to the initiator) of 1 N HCl solution. The precipitate obtained in diethyl ether was dialyzed against water and freeze-dried.

Ethylene oxide polymerization initiated with potassium pentaerythritolate was conducted with a similar method as described for three-arm PEO synthesis. Potassium pentaerythritolate (0.827×10^{-4} mol), which was previously pulverized and weighed in a nitrogen-purged glovebox, was placed in the reaction flask containing 20 mL of THF. After adding 10 mL (0.197 mol) of freshly distilled ethylene oxide, the reaction flask was kept for polymerization for 3 days at 40 °C. Termination and isolation were conducted with the same procedure as described previously.

Synthesis of Star-Shaped Poly(ether-ester) Block Copolymers. Star-shaped PEO-PLA and PEO-PCL block copolymers were prepared by ring-opening polymerization of L-lactide and ϵ -caprolactone, which was initiated with multiarm PEOs in the presence of stannous octoate as a catalyst. A reaction flask, which was equipped with a high-vacuum

stopcock, was connected to a vacuum line. Multiarm PEO (2 g) was placed in the reaction flask and was dehydrated by azeotropic distillation in benzene followed by further drying under vacuum at 120 °C for 1 h. A predetermined amount of L-lactide or ϵ -caprolactone and toluene solution of stannous octoate (0.1 mol % of the monomer) were added into the reaction flask. The toluene solution of stannous octoate (5% w/v) was prepared and the toluene was removed at room temperature under vacuum. After repeated evacuating and purging with argon gas, the reaction flask was finally evacuated to ca. 10 mmHg by a vacuum pump and then immersed in an oil bath preheated to 130 °C. Polymerization was carried out under stirring for 24 h at 130 °C. The reaction mixture was cooled to room temperature, dissolved in chloroform (ca. 50 mL), and precipitated into 1 L of cold methanol, diethyl ether, or their mixture to give a white product. The isolated polymer was dried at room temperature in vacuo.

Measurements. ^1H NMR and ^{13}C NMR spectra were recorded using a Bruker AS 200 FT spectrometer in CDCl_3 or $\text{DMSO}-d_6$ with tetramethylsilane (TMS) as an internal standard. For the quantitation of the terminal hydroxyl groups of PEO derivatives, NMR measurements were conducted in $\text{DMSO}-d_6$ as described in the literature.⁷

GPC was performed using a Waters liquid chromatography system equipped with Waters 501 Pump, 712 WISP autosampler, 745 Data Module, R401 differential refractometer, and a set of Ultrastaygel columns (linear and 500 Å pore size, Waters Co.). The sample, dissolved in tetrahydrofuran (THF), was injected at 25 °C with THF as an eluent at a flow rate of 0.5 mL/min. The sample concentrations were 0.5–1.0% w/v. Molecular weight and molecular weight distribution were calculated from calibration curves obtained from PEO and polystyrene standards (Polysciences Inc.). The standards have the relevant polydispersity indices (M_w/M_n) between 1.05 and 1.10, where M_w and M_n represent the weight- and number-average molecular weights, respectively.

The thermal transitions of the polymers were measured in aluminum pans using a differential scanning calorimeter (DSC, Perkin-Elmer DSC7). The thermograms covered a 30–200 °C temperature range at a 20 °C/min heating rate under nitrogen atmosphere. An indium standard was used to calibrate the temperature and the heat of fusion. The heat of fusion was determined by integrating the normalized area of melting endotherms.

Hydroxyl end groups of PEO derivatives were determined by visual titrimetric methods. An aqueous system was used because PEO derivatives were freely soluble in water. The distilled water used for dissolving the samples was boiled for a few minutes right before use. The hydroxyl groups were determined by an indirect method.⁸ Typically, an accurate amount of PEO derivatives (0.5 mequiv) was added into 10 mL of toluene solution containing acetyl chloride (1.5 mmol) and pyridine (2.45 mmol). After stirring for 20 min at 60 °C followed by adding 25 mL of water, the mixture was shaken thoroughly to hydrolyze excess acetyl chloride. The solution was titrated with 0.1 N sodium hydroxide in the presence of phenolphthalein as an indicator. A blank was run in parallel. The functionality (f , i.e., the number of hydroxyl end groups per one molecule of PEO derivatives), is given by

$$f = \frac{0.1(b - a) \text{ MW}}{1000 w(g)} \quad (1)$$

when w grams of PEO derivatives require a milliliters of 0.1 N sodium hydroxide. Then b and MW are the volume of titrant consumed for the blank and the molecular weight of the sample, respectively.

To study the swelling characteristics, polymer films (300–500 μm in thickness) were prepared by a solvent casting method using chloroform. The water content of the polymer was estimated gravimetrically by soaking the polymer films in distilled water at 37 °C. The specimens were periodically removed and weighed until equilibrium was attained. Samples were gently blotted prior to weighing to remove excess surface

water. The relative water uptake in percentage of dry weight was calculated according to

$$\text{water uptake (\%)} = \frac{W_{\text{wet}} - W_{\text{dry}}}{W_{\text{wet}}} \times 100 \quad (2)$$

where W_{wet} and W_{dry} represent the weight in wet and dry states.

Solution viscosity was measured at several flow rates in a Cannon-Fenske-type capillary viscometer. Measurement for PEO was conducted in distilled water at 35 °C and in methylene chloride at 25 °C for PEO-PLA and PEO-PCL block copolymers. Specific viscosity (η_{sp}) was obtained using eq 3

$$\eta_{\text{sp}} = t/t_0 - 1 \quad (3)$$

where t and t_0 are the outflow time for the solution and for the pure solvent, respectively.

For calculation of the intrinsic viscosity ($[\eta]$), Huggins equation⁹ was used

$$\eta_{\text{sp}}/C = [\eta] + k[\eta]^2 C \quad (4)$$

where C represents the concentration of the polymer solution (g/dL) and k is a constant for a given polymer at a given temperature in a given solvent.

Results and Discussion

Synthesis of Multiarm PEO. For the anionic polymerization of ethylene oxide, a highly reactive initiator and a polar solvent that allows high solvation of the cation are required to achieve a fast polymerization rate at temperatures slightly above ambient condition. For these reasons, potassium as a counterion and THF as a polymerization medium were used.

Trimethylolpropane was used as a starting material for the synthesis of three-arm PEO. Trimethylolpropane is soluble in THF; thus, the alcohols were transformed into potassium alkoxides by titration with an electron-transfer agent, potassium naphthylide, in THF. They reacted readily to completion at room temperature. The development of stable green color indicates that all hydroxyl groups have reacted and that there is a slight excess of potassium naphthylide. The alkoxide was freshly prepared prior to use because of its instability unless kept strictly under nitrogen atmosphere. The prepared alkoxide was precipitated as finely dispersed particles in THF.

For the preparation of four-arm PEO, Pentaerythritol was used. Since Pentaerythritol is not soluble in THF, potassium pentaerythritolate was synthesized by treating Pentaerythritol with an excess of *tert*-butoxide in *tert*-butyl alcohol. Potassium pentaerythritolate was isolated by precipitation in anhydrous diethyl ether and stored under nitrogen atmosphere. It was prepared immediately before use and handled in a glovebox purged with nitrogen. Since a fine suspension as trimethylolpropane could not be prepared, the *tert*-alkoxide was dispersed in the polymerization medium (THF) by pulverizing into fine particles.

Initially, the reaction medium remained heterogeneous, so the polymerization was conducted under vigorous stirring to prevent coagulation. Gradually, the reaction mixture became entirely homogeneous due to increased solubility of PEO in THF, indicating that most of the initiator was involved in the polymerization. Gradually, the reaction medium became viscous, partly owing to complexation between the alkoxides. The

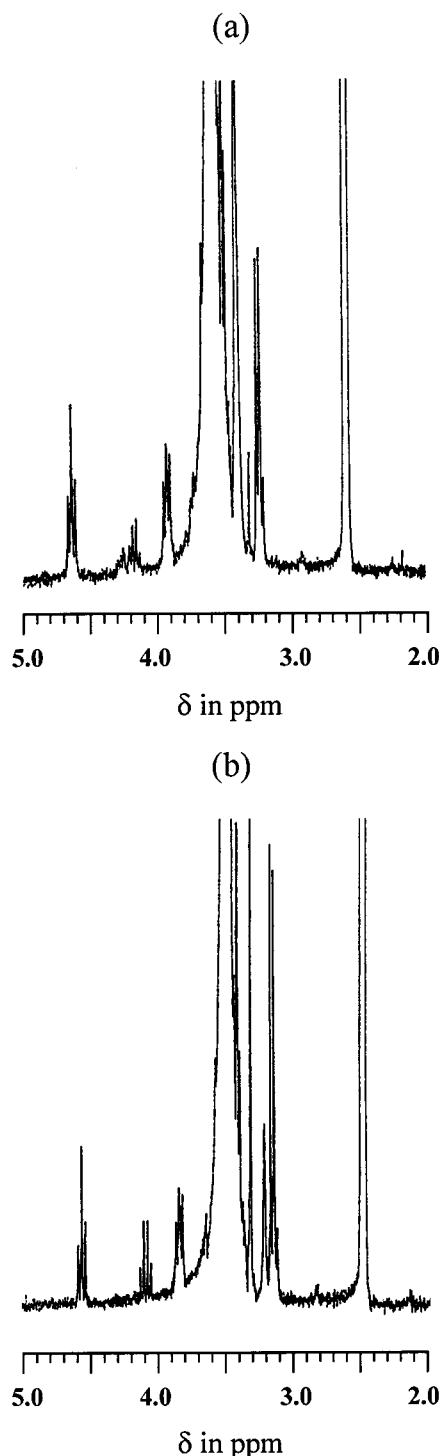


Figure 2. ^1H NMR spectrum ($\text{DMSO}-d_6$) of multiarm PEOs: (a) three-arm; (b) four-arm.

polymerization was conducted for 3 days, which was based on the time to reach the plateau value in the time-conversion experiment.

Figure 2 shows the ^1H NMR spectra of multiarm PEOs measured in $\text{DMSO}-d_6$. The hydroxyl protons at the PEO termini exhibit a clean triplet at $\delta = 4.56$ ppm in $\text{DMSO}-d_6$, which is separated from the large backbone peak ($\delta = 3.64$ ppm). Thus, it is possible to estimate the number of hydroxyl groups of PEO in a relatively low molecular weight PEO.⁶ However, in all spectra a chemical shift due to water was shown at $\delta = 3.32$ ppm, indicating that water had not been completely

Table 1. Experimental Results of Star-Shaped PEO Synthesis

no. of arms	M_w^a	M_n^b	polydispersity ^c (M_w/M_n)	no. of hydroxyl groups	
				calcd	measd (\pm SD) ^d
2	12 280	9 980	1.23	2.0	
3	9 760	9 480	1.03	3.0	3.07 ± 0.17
4	22 600	10 920	2.07	4.0	3.93 ± 0.26
8	20 240	10 070	2.01	8.0	7.62 ± 0.19

^a Weight-average molecular weights determined by GPC with PEO standards. ^b Number-average molecular weights determined by GPC with PEO standards. ^c Determined by GPC with PEO standards. ^d Determined by the indirect method using acetyl chloride; \pm SD represents the standard deviation ($n = 3$).

removed. Water may interact with hydroxyl protons at the polymer termini, hindering the quantification of the exact number of hydroxyl groups. The chemical shift at 4.08 ppm is due to the terminal methylene adjacent to hydroxyl group.

The experimental results of characterization of multiarm PEO are summarized in Table 1.

Synthesis of Star-Shaped PEO-PLA and PEO-PCL Block Copolymers. The ring-opening polymerization of L-lactide and ϵ -caprolactone was initiated with multiarm PEO in the presence of stannous octoate. Polymerization was conducted in bulk for rapid polymerization and high conversion, and the synthetic conditions used were for minimal ester interchange. Kim et al.¹⁰ reported the decrease of molecular weights at temperatures higher than 150 °C due to the transesterification reaction. Backbiting degradation was also reported at 150 °C when the polymerization lasted longer than 10 h. Accordingly, the reaction temperature was set at 130 °C, and the polymerization time was conducted for 20 and 10 h for L-lactide and ϵ -caprolactone, respectively. The conversions were over 95%.

The copolymers were characterized by ¹H NMR and GPC. Parts a and b of Figure 3 are ¹H NMR spectra with peak assignments of star-shaped PEO-PLA and PEO-PCL, respectively. They clearly show the formation of block copolymers. These assignments were made by comparison with literature data, as well as with spectra of binary mixtures based on PEO and PLA or PCL.

The block copolymerization was further confirmed by GPC measurements. In every cases star-shaped block copolymers showed sharp, unimodal distribution, indicating that the PEO had completely reacted with the L-lactide and ϵ -caprolactone, and no homopolymerization had occurred. The polydispersity indices ranged from 1.04 to 1.24. Although it was not clear whether all hydroxyl groups of multiarm PEO were involved in the initiation, it is probable that most of the hydroxyl end groups participated in the initiation because the initiation is nearly instantaneous.¹¹

Molecular weight, composition, and polydispersity are summarized in Table 2. These data show that block copolymers with the expected molecular weight and composition were obtained. The compositions and molecular weights were calculated from ¹H NMR spectra. They were determined by comparing the ratio of the PEO methylene ($\delta = 3.64$ ppm) integral, normalized to that for a single proton, to the average integral for the lactyl methine ($\delta = 5.16$ ppm) integral or caprolactone methylene ($\delta = 4.1$ ppm).

Swelling Behavior. The PEO contents were fixed at ca. 30% w/w for all samples. Water absorption

experiments presented in Figure 4 show swelling kinetic and equilibrium swelling of the block copolymers. For PLA (MW 20 000) and PCL (MW 20 000) homopolymers, equilibrium water contents were 2.7% and 0.4% w/w, respectively. The time-dependent water uptake profiles were biphasic (initial rapid water uptake followed by slow equilibration), and the equilibrium was attained within 30 min for both PEO-PLA and PEO-PCL block copolymers.

The equilibrium water content decreased with increased number of arms of the block copolymers with similar polymer compositions and molecular weights, indicating that the magnitude of water uptake depends on the molecular architecture. This effect may be attributed to a difference in local average polymer density which increases with higher branching. A light scattering study has shown that the swelling of star-shaped polymers is consistent with a model of an impenetrable core from which the arms of the star radiate outward.¹² Another factor that influences the swelling is the phase mixing of the PEO segments with PLA or PCL segments. As the number of arms increases, the shorter PEO may have preferential interaction with PLA or PCL segment via increased number polar end groups of the PLA or PCL, resulting in enhanced miscibility between two phases (see the next section). It was observed that the water content of PEO-PLA block copolymers was higher than that of PEO-PCL block copolymers at the same molecular weight, star architecture, and PEO contents. This is due to the more hydrophobic nature and higher crystallinity of PCL compared to PLA blocks.

Thermal Property. Figure 5 represents the DSC thermograms of multiarm PEOs. The melting points (T_m) of the three-, four-, and eight-arm PEOs were observed at 55.5, 49.1, and 40.7 °C, respectively, whereas that of two-arm (linear) PEO appeared at 63.1 °C (Table 3). The melting point gradually shifted to lower temperatures as the number of arms increased. The reduced melting point with branching is attributed to decrease in chain length, and thus increased free chain ends, probably disrupting the orderly fold pattern of the crystal.

It was noted that melting peak was broadened as the degree of branching increased. The quantity ΔT_m is related to the dispersion of the crystal thickness, which depends on the conditions of crystallization, annealing, molecular length, polydispersity, and the measurement conditions. At the same experimental conditions and with nearly constant molecular weight and polydispersity of multiarm PEOs which are presented in Table 1, the branching effect might be a crucial factor in determining the melting process. Many defects which are observed more in the higher branched PEO must decrease the interchain cooperativity, resulting in the broadening of melting range.¹³

The heats of fusion (ΔH_m) are shown in Table 3. Gradual decrease in ΔH_m was noticed as the number of arms increased. The increased disturbance in order due to a larger number of end groups and branching will result in less intermolecular interaction, which becomes the decreasing function of ΔH_m .¹⁴ From the measured value of ΔH_m of multiarm PEOs, the degree of crystallinity (χ_c) was calculated according to eq 5

$$\chi_c = \Delta H_m / \Delta H_m^\infty \quad (5)$$

Table 2. Results of L-Lactide and ϵ -Caprolactone Polymerization Initiated by Star-Shaped PEO in Bulk at 130 °C

code	structure	PEO in feed		copolymer MW ^a			polydispersity ^b (M_w/M_n)
		MW ^a	wt %	calcd	¹ H NMR	GPC	
PELA 2S	2-arm star-shaped PEO-PLA block	9 980	30.0	33 230	31 710	29 150	1.08
PELA-3S	3-arm star-shaped PEO-PLA block	9 760	30.0	32 530	31 460	26 140	1.12
PELA-4S	4-arm star-shaped PEO-PLA block	10 920	30.0	36 400	38 690	28 460	1.12
PLLA-8S	8-arm star-shaped PEO-PLA block	10 000	30.0	33 300	31 185	34 530	1.24
PECL-2S	2-arm star-shaped PEO-PCL block	9 980	30.0	33 230	35 210	49 120	1.04
PECL-3S	3-arm star-shaped PEO-PCL block	9 760	30.0	32 530	34 620	35 940	1.05
PECL-4S	4-arm star-shaped PEO-PCL block	10 920	30.0	36 400	38 353	40 080	1.14
PECL-8S	8-arm star-shaped PEO-PCL block	10 000	30.0	33 300	42 695	56 080	1.10

^a Number-average molecular weights. ^b Measured by GPC with PEO standards.

where ΔH_m is the heat of fusion of a sample and ΔH_m^∞ is the theoretical heat of fusion of homopolymers at 100% crystallinity. ΔH_m^∞ (206.2 J/g) for PEO was obtained from the average value shown in the literature.¹⁵ For the two-arm PEO, the degree of crystallinity was calculated as 85.9%. The crystallinity was reduced further as the branching increased (Table 4). The smaller value of the entropy of fusion (ΔS_m), calculated from the eq 6,¹⁶ in more branched PEO is

$$\Delta S_m = \Delta H_m / T_m \quad (6)$$

attributed to the restricted conformation, owing to the increased degree of branching (Table 3).

Figure 6 shows the DSC thermograms of the star-shaped PEO-PLA block copolymers. Their transition temperatures are summarized in Table 4. The PEO-PLA block copolymer films were all opaque, indicating the phase separation, while the homo-PLA film is translucent. However, T_g 's were not observed in the DSC for PEO-PLA block copolymers due to overlapping of the T_g of PLA (40–60 °C)^{17,18} with the melting point of PEO. The endotherm is ascribed to the crystal fusion of PLA segments which was observed at temperatures lower than the melting point of PLA around 173 °C (data not shown). This fact indicates that the crystallization of PLA blocks is disturbed by the existence of PEO blocks. The melting points were decreased as the number of arms increased (Table 3). Considering the constant PEO content of star-shaped block copolymers, this lowered melting points are due to the star architecture. For the eight-arm star-shaped PEO-PLA block copolymer (Figure 6d), two melting peaks were observed. The two melting endotherms can be observed often in partially crystalline polymers. This phenomenon is generally considered: (1) reorganization of metastable crystals from folded chains and (2) recrystallization of folded chain crystals.¹⁹ A similar phenomenon has been found in the linear PEO-PLA block copolymer and has been interpreted by the crystallites of different size and different degree of perfectionness.¹⁶

The heat of fusion (ΔH_m) of PLA segments in the block copolymers is lower than the value reported for PLA. For example, the ΔH_m of PLA segment of four-arm block copolymers (31.38 J/g) is much lower than the value of 61 J/g reported for a PLA of similar molecular weight (5300 g/mol).²⁰ This difference may be attributed to the

central PEO block which tends to limit the crystal thickness and perfection. The ΔH_m was further decreased as the number of arms increased, indicating the presence of an architectural factor as previously described.

The degree of crystallinity (χ_c) of PLA segments was calculated using eq 5 and is presented in Table 4. The ΔH_m^∞ value (92.84 J/g) for a perfect PLA crystal was obtained from the literature.²¹ The calculated value of χ_c was in the range of 8.1–40.3%. The crystallinity of PLA segments increases with their segmental length. The weight fractions of crystalline PLA segments were calculated with the consideration of polymer composition and are shown in Table 4.

No endothermic melting peak of PEO was observed in all star-shaped PEO-PLA block copolymers, indicating that PEO segments were phase-mixed with the PLA. One of melting endotherms in the block copolymers can be lost when the block length is relatively short and the content is relatively low. This is consistent with the results in the literature which observed that melting peak of the PEO segments disappears and crystallinity of PEO segments approaches to zero, when the molar ratio of the PEO segments is lower than 40% in the PEO-PLA block copolymer.²² The PEO melting endotherm has not been detected even at 62 mol % of PEO in the first run of DSC.²³ It has also been reported that the PLA segments have higher tendency in retaining their crystalline array than the PEO segments.²⁴ The PLA hard segments are the first to solidify upon cooling, hindering the mobility of soft PEO segments. As a result, the crystallization of the PEO segments is hampered, especially in a block copolymer with small content of PEO. In this study, the DSC thermograms were obtained from first scanning of the powdered sample. However, isothermal PEO recrystallization from the polymer melt is expected due to reorganization. It was reported that the PEO melting endotherm of PEO-PLA copolymer was detected after annealing, and the enthalpy of melting process was shown to increase with the annealing time.^{16,23,25} Even with various segmental lengths, the star-shaped PEO-PLA block copolymers reveal PLA crystalline domains, probably lamellar structures dispersed in an amorphous continuous phase formed by intermingled PEO and PLA. The observed exothermic peaks at 90–95 °C are related to the crystallization of the PLA segments, as reported in

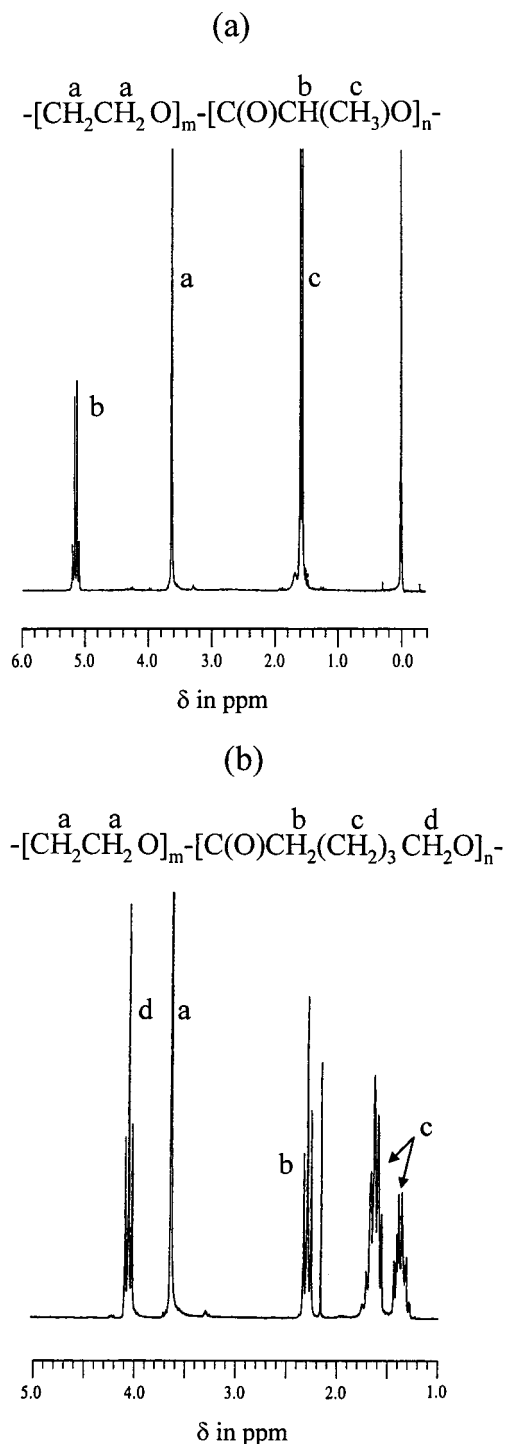


Figure 3. ^1H NMR spectrum (CDCl_3) of (a) three-arm star-shaped PEO-PLA and (b) three-arm star-shaped PEO-PCL block copolymers.

the literature.^{22,25,26} A smaller change of the crystallization temperature (T_c) was observed compared to the melting temperature change.

The DSC thermograms of star-shaped PEO-PCL copolymers without any thermal treatment are presented in Figure 7. Thermodynamic parameters, including thermal transition temperatures, are shown in Table 3. The crystallinity of PCL segments is presented in Table 4, which was calculated using a ΔH_m value (135 J/g) of PCL in the literature.²⁷ The DSC thermograms of PEO-PCL block copolymers exhibit two melting endotherms, which are characteristic thermal transi-

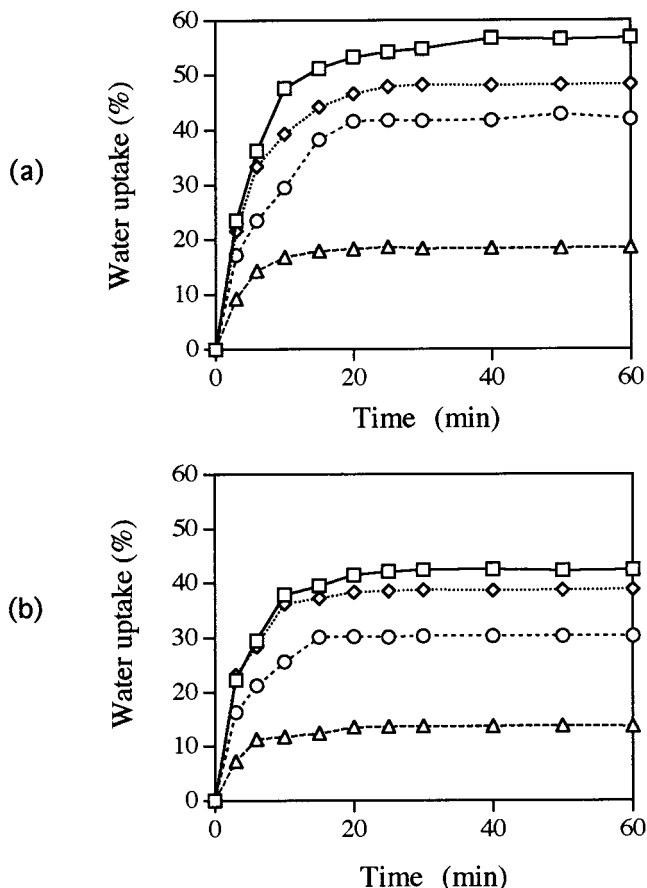


Figure 4. Swelling kinetics of star-shaped (a) PEO-PLA and (b) PEO-PCL block copolymers: \square , two-arm; \diamond , three-arm; \circ , four-arm; \triangle , eight-arm.

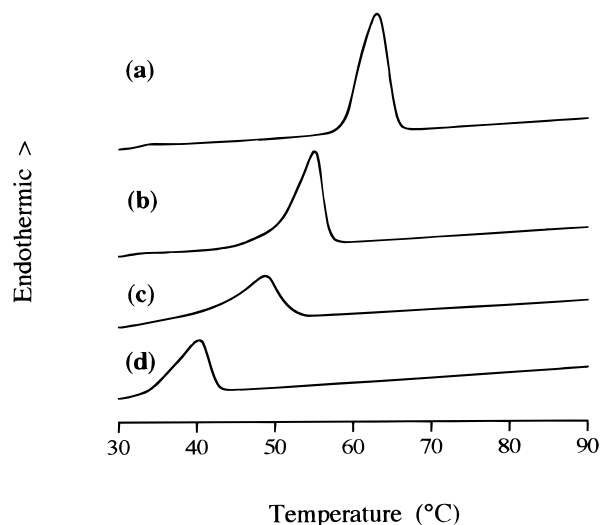


Figure 5. DSC thermograms of star-shaped PEO 10000 (heating rate $20^\circ\text{C}/\text{min}$): (a) two-arm; (b) three-arm; (c) four-arm; (d) eight-arm.

tions of PEO and PCL segments. This phenomenon indicates that two immiscible PEO and PCL phases are separately present. It is noteworthy that the PEO melting endotherm appeared in the DSC thermograms of PEO-PCL block copolymers, in contrast to the results from PEO-PLA block copolymers of similar PEO contents and molecular architecture. This finding clearly indicates that PEO is more miscible with PLA than with PCL. However, from the decrease in melting point and

Table 3. Thermal Transition Temperatures and Thermodynamic Parameters of Star-Shaped Polymers

polymer sample	PEO (wt %)	T_m (°C)			ΔH_m (J/g)			ΔS_m (J/g °C) ^a		
		PEO	PLA	PCL	PEO	PLA	PCL	PEO	PLA	PCL
PEO-2S	100.0	63.05			177.06			2.81		
PEO-3S	100.0	55.47			152.98			2.75		
PEO-4S	100.0	49.12			124.83			2.54		
PEO-8S	100.0	40.72			97.47			2.39		
PELA-2S	31.48		158.35			37.42			0.236	
PELA-3S	31.02		156.70			36.15			0.231	
PELA-4S	28.22		155.03			31.38			0.202	
PELA-8S	32.07		134.20			7.50			0.056	
PECL-2S	28.34	48.28		61.11	28.06		51.28	0.581		0.839
PECL-3S	28.19	43.94		60.64	25.26		50.32	0.575		0.829
PECL-4S	28.47	43.16		58.58	7.90		64.36	0.183		1.099
PECL-8S	23.42			53.12			70.50			1.327

^a Calculated from the thermodynamic relationship $\Delta S_m = \Delta H_m/T_m$.

Table 4. Degree of Crystallinity (χ_c) of Star-Shaped Polymers

polymer sample	PEO (wt %)	T_c (°C)	ΔH_{cryst} (J/g)	χ_c^a			% crystallization ^b		
				PEO	PLA	PCL	PEO	PLA	PCL
PEO-2S	100.0			0.859					
PEO-3S	100.0			0.742					
PEO-4S	100.0			0.605					
PEO-8S	100.0			0.473					
PELA-2S	31.48	92.97	15.70		0.403			27.61	
PELA-3S	31.02	94.57	13.93		0.389			26.83	
PELA-4S	28.22	94.81	14.82		0.338			24.26	
PELA-8S	32.07	90.50	17.76		0.081			5.49	
PECL-2S	28.34			0.136		0.380	3.85		27.23
PECL-3S	28.19			0.123		0.373	3.46		26.79
PECL-4S	28.47			0.038		0.476	1.08		34.10
PECL-8S	23.42					0.522			39.90

^a Degree of crystallinity $\chi_c = \Delta H_{m,\text{sample}}/\Delta H_{m,100\%}$, 100% crystalline. ^b Weight fraction in copolymer which is crystalline, $\chi_c \times (\text{wt } \%)$.

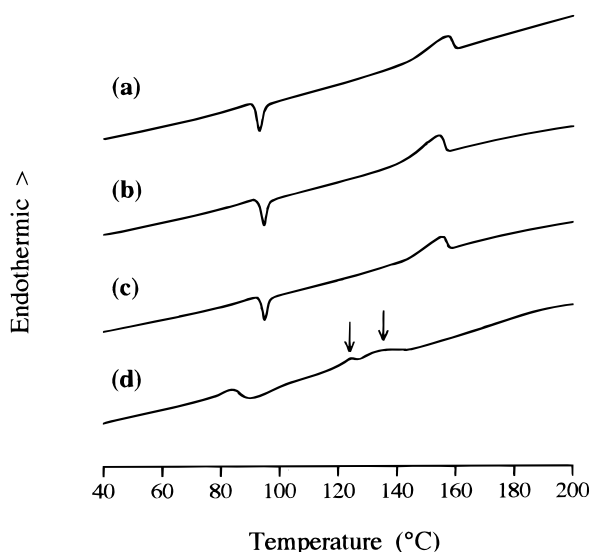


Figure 6. DSC thermograms of star-shaped PEO-PLA block copolymers prepared from ca. 30 w/w % of PEO 10000: (a) two-arm; (b) three-arm; (c) four-arm; (d) eight-arm.

crystallinity of PEO segments (Tables 3 and 4), it becomes evident that PEO segments are partially miscible with PCL segments. The PEO crystallinities of two-, three-, and four-arm block copolymers were reduced to only 15.8, 16.6, and 8.0% of those of PEO homopolymers, respectively. This fact indicates that considerable phase mixing has taken place, and the mixing extent increases with the number of arms in the PEO-PCL block copolymers. The PCL crystalline imperfection due to phase mixing also caused a decrease in the PCL melting point. Therefore, in the PEO-PCL

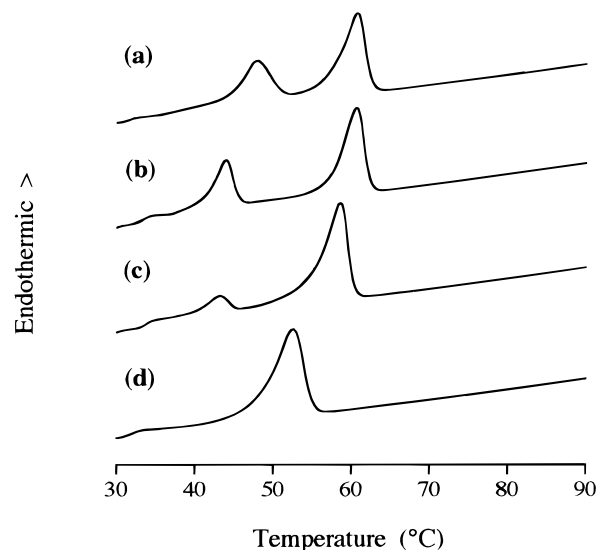


Figure 7. DSC thermograms of star-shaped PEO-PCL block copolymers prepared from ca. 30 w/w % of PEO 10000: (a) two-arm; (b) three-arm; (c) four-arm; (d) eight-arm.

block copolymers the two crystalline PEO and PCL domains are assumed to be separated by amorphous interfacial regions, where phase mixing occurs. When the number of arms in a PEO-PCL block copolymer is eight, PEO segments failed to crystallize because of the substantial increase in the number of end groups and decrease in segmental length, resulting in the consequent disappearance of the PEO melting endotherm (Figure 7d).

Solution Property. Specific viscosities of the multiarm PEO and block copolymers in water were mea-

Table 5. Intrinsic Viscosities and Their Ratios for Star-Shaped PEO, PEO-PLA, and PEO-PCL Block Copolymers

polymer	f^a	$[\eta]^b$ (dL/g)	g'_{exp}^c
PEO-2S	2	0.184	1.000
PEO-3S	3	0.150	0.815
PEO-4S	4	0.090	0.489
PEO-8S	8	0.047	0.255
PELA-2S	2	0.381	1.000
PELA-3S	3	0.310	0.814
PELA-4S	4	0.206	0.541
PELA-8S	8	0.182	0.478
PECL-2S	2	0.806	1.000
PECL-3S	3	0.573	0.711
PECL-4S	4	0.479	0.594
PECL-8S	8	0.435	0.540

^a Number of arms. ^b Measured in distilled water at 35 °C for PEO and in methylene chloride at 25 °C for PEO-PLA and PEO-PCL block copolymers. ^c $g'_{\text{exp}} = [\eta]_{\text{star}}/[\eta]_{\text{linear}}$ by definition.

sured and plotted using the Huggins equation in order to obtain zero-shear rate intrinsic viscosity $[\eta]$. The comparison of intrinsic viscosities and the ratio of $g'_{\text{exp}} = [\eta]_{\text{star}}/[\eta]_{\text{linear}}$ are made in Table 5. The results showed that more branched PEO showed lower intrinsic viscosity with the same number-average molecular weight as expected. Because the intrinsic viscosity is related to the mean-square radius of gyration by Flory's relationship¹³

$$[\eta] = \frac{6^{3/2} \Phi \langle S^2 \rangle^{3/2}}{M_w} \quad (7)$$

where $\langle S^2 \rangle$ is the mean-square radius of gyration and Φ is the universal constant, the lower intrinsic viscosity of the polymers with the same molecular weight reply the smaller radius of gyration.

In this study, to obtain information about the effect of branching on molecular dimension, the value of g'_{exp} was determined and compared with the theoretical predictions proposed by Zimm and Kilb²⁸ and by Stockmayer and Fixman.²⁹ Zimm and Kilb derived the relation of

$$g' = g^{1/2} \quad (8)$$

for all star-shaped molecules, where g (branching factor) = $\langle S^2 \rangle_{\text{star}}/\langle S^2 \rangle_{\text{linear}}$ at θ -conditions. The theoretical g value has been shown to be given by

$$g_{\text{theo}} = (3f - 2)/f^2 \quad (9)$$

for regular star polymers of equal molecular weight, where f denotes the number of arms in the molecule.³⁰ Independently, Stockmayer and Fixman calculated the shrinking factor, h , from the ratio of frictional constant ($[F]$) of star branched polymer to that of the linear polymer of the same molecular weight

$$\eta = \frac{[F]_{\text{star}}}{[F]_{\text{linear}}} = \frac{\sqrt{f}}{2 - f + \sqrt{2}(f - 1)} \quad (10)$$

and extended this to the intrinsic viscosity by the approximation

$$h^3 = [\eta]_{\text{star}}/[\eta]_{\text{linear}} \quad (11)$$

The theoretically predicted values of g' for three-, four-, and eight-arm polymers are 0.882, 0.791, and 0.586, respectively. For h^3 , the values are 0.850, 0.709, and 0.392, respectively. The experimental value of g'_{exp} appeared to be smaller than the calculated one and decreased more rapidly with branching than those predicted by theories (eqs 9–11). This result may be due to the deviation of experimental conditions (water at 35 °C for PEO and methylene chloride at 25 °C for the block copolymers: good solvent conditions) from the θ -condition. Polymer chains become fully extended in a good solvent due to the favorable intermolecular interaction between polymer and solvent rather than intramolecular interaction between homologues. The attractive force between polymer chains and water results in the increase in the average end-to-end distance. In contrast, all theoretical considerations are under strict θ -conditions, where the intermolecular polymer-liquid interaction is equivalent to intramolecular interactions. A bulkier linear chain is more significantly affected by a polymer-solvent interaction, whereas a highly branched polymer with compact packing is less dependent on the solvent quality. Since the g' value is expressed by relative dimension of a branched polymer to a linear one, the dependence of g' value on branching becomes larger in a good solvent. That is, a net attractive force prevails between copolymer and solvent due to the good solvent quality of methylene chloride for both block copolymers. Thus, the polymer chain will expand until opposing enthalpic and entropic forces are in balance, resulting in the increase in the average end-to-end distance.

Conclusions

Star-shaped PEO-PLA and PEO-PCL block copolymers composed of identical polymer branches were synthesized to investigate swelling behavior, thermal property, and solution property. The block copolymers formed swollen hydrogel in distilled water. The hydrophobic PLA or PCL domain acted as a physical cross-linking point. The degree of swelling decreased as the number of arms increased due to (1) more compact packing in higher branched star polymers and (2) the decreased PEO domain size and greater phase mixing of PEO with the polyester block in higher branched copolymers.

The thermal properties showed the branching effect on polymer structure, as well as the interesting morphological features of physically cross-linked block copolymers. The melting point (T_m) and heat of fusion (ΔH_m) of star-shaped PEO, PEO-PLA, and PEO-PCL polymers decreased with the degree of branching. In particular, low T_m was noted in the case of the highly branched PEO-PCL block copolymer. Since the melting point is related to crystalline structure and size, the decrease in T_m is attributed to the crystalline imperfections due to increased end groups and branching points in the more branched polymers. The decrease in ΔH_m is due to the decrease in the degree of crystallinity with branching. The polymer matrix of eight-arm PEO-PLA is predicted to be almost amorphous from the absence of melting of PEO and the very small degree of PLA crystallinity (8.1%). In contrast, phase separation was noticed in the PEO-PCL, in which the degree of PEO crystallinity was decreased with the degree of branching. Branching hinders microphase separation due to the increase in end groups and branching points.

The intrinsic viscosity of star-shaped polymers was decreased with degree of branching. The smaller value of g'_{exp} compared to the theoretical predictions was observed since the good solvent in the viscosity measurement makes polymer chains fully extended due to the thermodynamically favorable interactions between polymer and solvent. Particularly high dependence of g' on branching is noted in the case of multiarm PEO. The smaller molecular dimension of PEO is of importance for the complete renal excretion after degradation of an implanted polymer matrix.

These results are basically derived from the distinct molecular architecture of star-shaped polymers and may subsequently influence the formulation, drug loading, and in vivo fate of drug and polymers. The modified intrinsic viscosity of star-shaped block copolymers can be expected to affect the particle size and drug loading in the design of microparticulate systems. The changed swelling and morphology, due to branching, may affect the drug release profiles.

Acknowledgment. This work was supported by NIH Grant GM 56098-01.

References and Notes

- (1) Casey, D. J.; Jarrett, P. K.; Rosati, L. U.S. Patent 4,716,203.
- (2) Cohn, D.; Younes, H. *J. Biomed. Mater. Res.* **1988**, *22*, 993.
- (3) Youxin, L.; Volland, C.; Kissel, T. *J. Controlled Release* **1994**, *32*, 121.
- (4) Choi, Y. K.; Bae, Y. H.; Kim, S. W. *Proc. Int. Symp. Control. Relat. Bioact. Mater.* **1996**, *23*, 349.
- (5) Perrin, D. D.; Armarego, W. L. F. *Purification of Laboratory Chemicals*, 3rd ed.; Pergamon Press: Oxford, 1988.
- (6) Morton, M.; Milkovich, R. *J. Polym. Sci., Part A* **1963**, *1*, 443.
- (7) Dust, J. M.; Fang, Z.; Harris, J. M. *Macromolecules* **1990**, *23*, 3742.
- (8) Veibel, S. Recommended methods for the estimation of hydroxy compounds. In *The Determination of Hydroxyl Groups*; Veibel, S., Ed.; Academic Press: New York, 1972; pp 113–147.
- (9) Rabek, J. F., Ed. *Experimental Methods in Polymer Chemistry-Physical Principles and Applications*; John Wiley & Sons: New York, 1980.
- (10) Kim, S. H.; Han, Y.-K.; Kim, Y. H.; Hong, S. I. *Makromol. Chem.* **1992**, *193*, 1623.
- (11) Schindler, A.; Hibionada, Y. M.; Pitt, C. G. *J. Polym. Sci., Polym. Chem. Ed.* **1982**, *20*, 319.
- (12) Birshtein, T. M.; Zhulina, E. B.; Borsov, O. V. *Polymer* **1986**, *27*, 1078.
- (13) Wunderlich, B., Ed. *Macromolecular Physics*; Academic Press: New York, 1973, 1976, 1980; Vols. 1–3.
- (14) Flory, P. J., Ed. *Principle of Polymer Chemistry*; Cornell University Press: Ithaca, NY, 1953.
- (15) Brandruo, J.; Emmergut, E. H., Eds. *Polymer Handbook*, 3rd ed.; John Wiley & Sons: New York, 1989; pp VI-72.
- (16) Liu, H.-J.; Hu, D. S.-G. *Makromol. Chem.* **1993**, *194*, 3393.
- (17) Kricheldorf, H. R.; Meier-Haack, J. *Makromol. Chem.* **1993**, *194*, 715.
- (18) Shah, S. S.; Zhu, K. J.; Pitt, C. G. *J. Biomater. Sci. Polym. Ed.* **1994**, *5*, 421.
- (19) Bershtein, V. A.; Egorov, V. M., Eds. *Differential Scanning Calorimetry of Polymers-Physics, Chemistry, Analysis, and Technology*; Ellis Horwood Ltd.: New York, 1994.
- (20) Celli, A.; Scandola, M. *Polymer* **1992**, *33*, 2699.
- (21) Brandruo, J.; Emmergut, E. H., Eds. *Polymer Handbook*, 3rd ed.; John Wiley & Sons: New York, 1989; p VI-62.
- (22) Youxin, L.; Kissel, T. *J. Controlled Release* **1993**, *27*, 247.
- (23) Jedlinski, Z.; Kurcok, P.; Walach, W.; Janeczek, H.; Radecka, I. *Makromol. Chem.* **1993**, *194*, 1681.
- (24) Younes, H.; Cohn, D. *J. Biomed. Mater. Res.* **1987**, *21*, 1301.
- (25) Bachari, A.; Belorgey, G.; Helary, G.; Sauvet, G. *Macromol. Chem. Phys.* **1995**, *196*, 411.
- (26) Kimura, Y.; Matsuzaki, Y.; Yamane, H.; Kitao, T. *Polymer* **1989**, *30*, 1342.
- (27) Brandruo, J.; Emmergut, E. H., Eds. *Polymer Handbook*, 2nd ed.; Wiley: New York, 1975; p III-33.
- (28) Zimm, B. H.; Kilb, R. H. *J. Polym. Sci.* **1959**, *37*, 19.
- (29) Stockmayer, W. H.; Fixman, M. *Ann. N.Y. Acad. Sci.* **1953**, *57*, 334.
- (30) Zimm, B. H.; Stockmayer, W. H. *J. Chem. Phys.* **1949**, *17*, 1301.

MA981069I